

# Supplemental Material

## Characterizing chaos in systems subjected to parameter drift

Dániel János, Tamás Tél

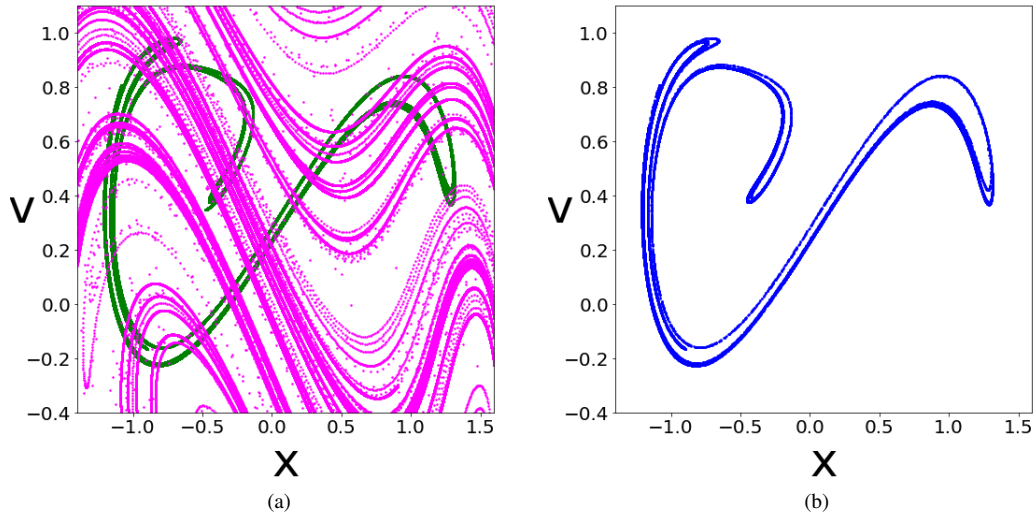


Figure S1: Snapshot chaotic horseshoe of a snapshot attractor with space filling snapshot stable foliation. Here, we chose a scenario with larger  $\varepsilon_0$  and  $\beta$  values:  $\varepsilon_0 = 0.5$ ,  $\alpha = 0.0005$ ,  $\beta = 0.2$ ,  $\omega = 1$ . This scenario scans a parameter range of the bifurcation diagram of the drift-free case (see Fig. S2) in which chaotic attractors exist intermingled with periodic windows. By the end it had already passed such a window, nevertheless, the snapshot attractor can be observed not to change its structure dramatically throughout the whole scenario. In panel (a) we show the snapshot chaotic horseshoe with the unstable foliation in green and the stable one in pink, for  $n = 25$  and  $k = 5$ . Five initial segments of length  $dl = 0.2$  are used for the initialization of the foliation, centered at  $(-1, 0.8)$ ,  $(-0.5, -0.2)$ ,  $(0, 0.25)$ ,  $(0.5, 0.2)$ ,  $(1, 0.7)$ , each containing  $N = 500000$  points. We can clearly see that the stable foliation spreads out to the whole phase plane. Although the shading is not uniform, the pattern is rather similar to those obtained with finite-time integrations for the stable manifold of traditional chaotic attractors, which are known to be asymptotically space filling. As a consequence, here the chaotic saddle is *dense* along the unstable foliation. This is in contrast to the case in Fig.2 of the main text, where the existence of the SNPs restricts the area that the snapshot stable foliation can occupy, but here there is no such restriction: in this scenario no regular snapshot attractors (SNPs) exist. Because of the strong phase space explosion in backward iterations due to the relatively large value of  $\beta$ , in order to get a representative picture, we constructed the image using an augmentative approach: in each step, we initiated new segments (the same ones as above), and used the filaments originating from them to augment the already existing snapshot foliation. Without this method, the points would have very quickly left the investigated area. In panel (b) we show the strange snapshot attractor of this scenario at  $n = 25$ , initiated from a square of side length 0.8 centered at the origin, containing  $N = 40000$  points. Comparing it to the unstable foliation in (a), it is clear that the two are approximately identical, just like the ones in Fig.1. Here, because of the lack of regular attractors, the entire strange snapshot attractor is chaotic, thus, to distinguish it from the case studied in the main text, such snapshot attractors can be called *chaotic snapshot attractors*.

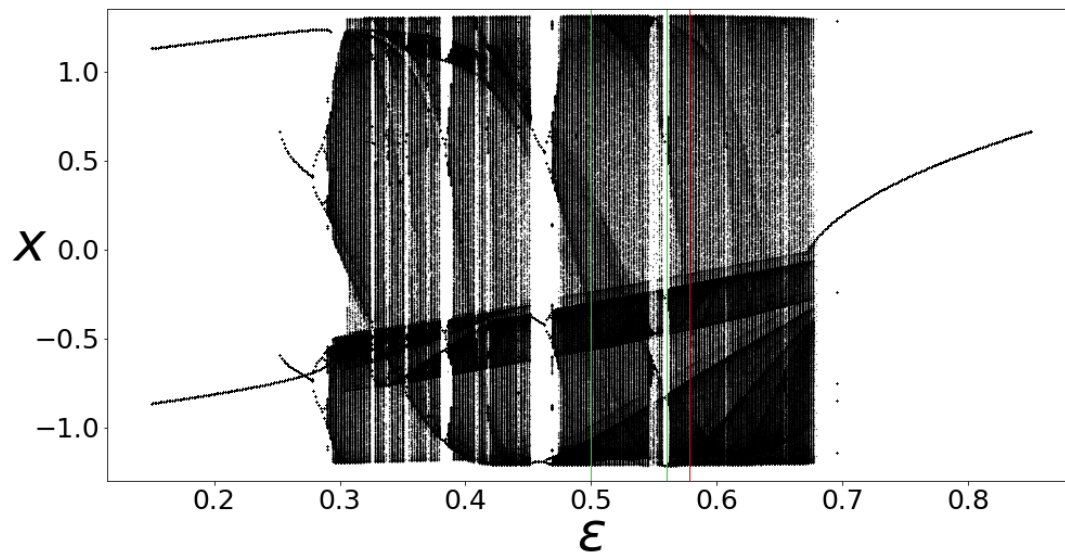


Figure S2: Bifurcation diagram of the drift-free Duffing system according to the  $\varepsilon$  amplitude, with damping coefficient  $\beta = 0.2$  and frequency  $\omega = 1$ . As one can see, it exhibits both period-doubling and crisis-type bifurcations at  $\varepsilon \approx 0.29$ , from which point both chaotic regions and periodic windows occur. The start of the scenario shown in Fig. S1 ( $\varepsilon = 0.5$ , first green line) is in a chaotic regime, and by the end ( $\varepsilon \approx 0.578$ , red line) the scenario has already gone through a parameter region corresponding to a periodic window (around  $\varepsilon = 0.56$ , second green line). The character of the snapshot attractor, and of the unstable foliation, can be observed to be the same as that of Fig. S1 throughout the scenario, not changing even in the region corresponding to the periodic window. Thus we can say that snapshot attractors typically do not go through sudden structural changes, i.e. crises. The fact that the bifurcation diagram of the drift-free system is not followed in the drifting one by the snapshot attractor - provided the change is not adiabatic - was already pointed out in [25].

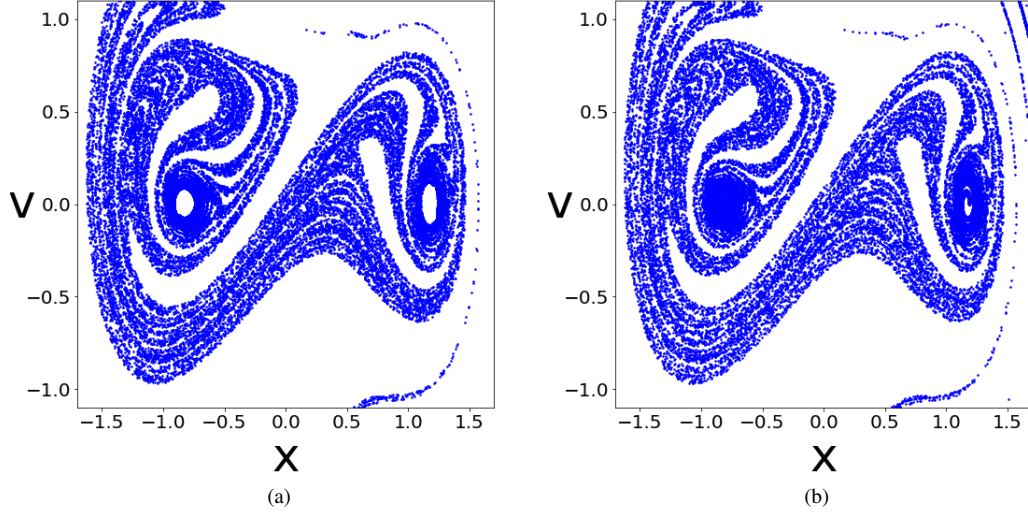


Figure S3: Strange snapshot attractor in the scenario  $\varepsilon = 0.08$ ,  $\alpha = 0.0005$ ,  $\beta = 0.01$ ,  $\omega = 1$  (the same as in Fig.1 of the main text), without the cut-out around  $\pm 1$ . (a) The exact same picture as Fig.1d, but without the cut-out. We can clearly see the spiraling pattern towards the SNPs. (b) The snapshot attractor but with a larger initial ensemble, that being a distribution of points on a square of side length 2 centered at the origin. This was chosen in order to demonstrate that the strange snapshot attractor does indeed contain the SNPs within itself. Note that despite the differences in the compact regions, the filamentary pattern is practically the same in both, also coinciding with the filamentary part of the snapshot unstable foliation.

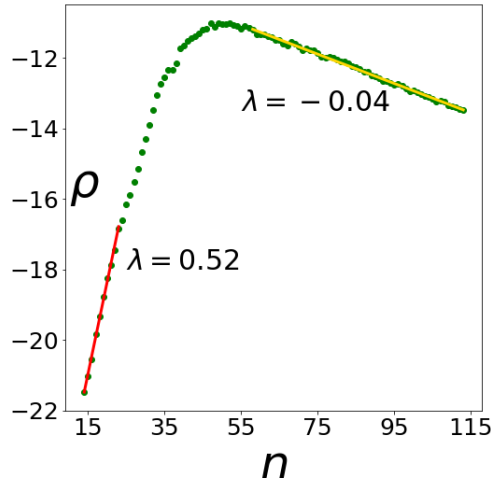


Figure S4: The strength of chaos in a strange snapshot attractor whose simulation is initiated at  $n = 10$  (and not  $n = 0$ ) in the same scenario than that of Fig.4a of the main text. The evaluation of the EAPD starts at  $n = 15$ , at which point the convergence time has just passed. This setup is chosen because this way the least possible amount of points should end up near the SNPs, since these skew the average pairwise distance towards smaller values. Despite this, as one can clearly see, the initial positive Lyapunov exponent still ends up being slightly smaller than that of Fig.4a, which can be attributed to the snapshot attractor approaching the SNPs faster than the snapshot unstable foliation. Nevertheless, the maxima and the overall shapes of the two curves are indeed similar.

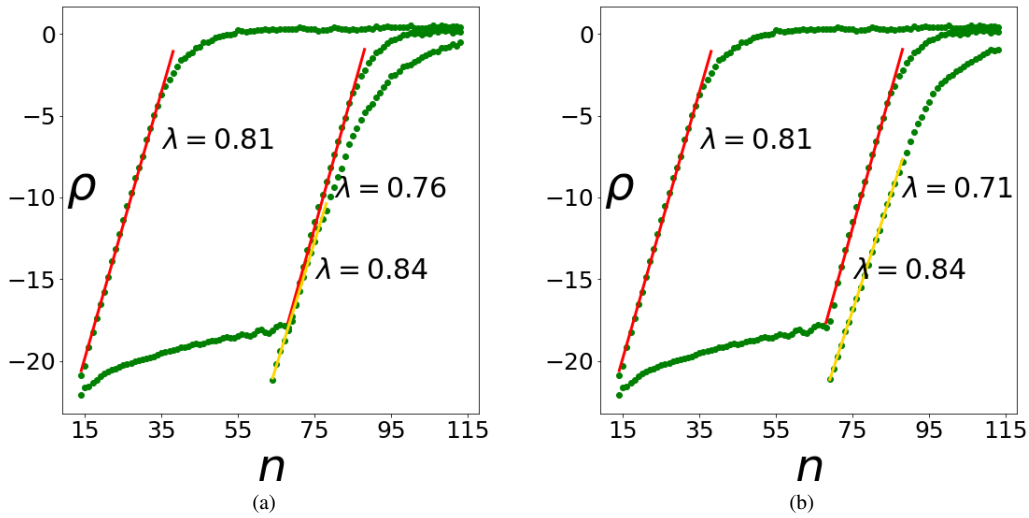


Figure S5: The same image as Fig.4b, but with one additional EAPD curve (whose initial slope is marked by a yellow line) representing a snapshot chaotic sea started at  $n = 15$ . In panel (a) the evaluation of the EAPD for this set is started at  $n = 65$ , because this is the point where the fitted line of the curve of the snapshot torus crosses  $\rho \approx -22$ , the value corresponding to the initial distances. This way, if the Lyapunov exponent of the snapshot chaotic sea is the same as that of the torus, then the two curves should lie on top of each other. In panel (b), the evaluation is started at  $n = 70$ , the point of the breakup; here equal Lyapunov exponents would mean that the two curves are parallel. These new curves indeed turn out to be similar to that of the snapshot torus (from the point of the breakup), however with a slightly smaller Lyapunov exponent. This might be explained by the fact that the snapshot chaotic sea could contain areas (close to not yet broken up snapshot tori) that are less chaotic than other parts of the snapshot chaotic sea.